

Next-to-leading order QCD calculations with parton showers II: soft singularities

Davison E. Soper

Institute of Theoretical Science, University of Oregon, Eugene, OR 97403 USA
(Dated: 26 June 2003)

Abstract

Programs that calculate observables in quantum chromodynamics at next-to-leading order typically generate events that consist of partons rather than hadrons (and just a few partons at that). These programs would be much more useful if the few partons were turned into parton showers, which could be given to one of the Monte Carlo event generators to produce hadron showers. In a previous paper, we have seen how to generate parton showers related to the final state collinear singularities of the perturbative calculation for the example of $e^+ + e^- \rightarrow 3$ jets. This paper discusses the treatment of the soft singularities.

arXiv:hep-ph/0306268v2 15 Aug 2003

I. INTRODUCTION

This is the second of two papers concerning how to modify a next-to-leading order (NLO) calculation in quantum chromodynamics by adding parton showers in such a way that when the generated events are used to calculate an infrared safe observable, the observable is calculated correctly at next-to-leading order. In the companion paper [1], M. Kramer and the present author explain the aspects of this problem that relate to the divergences that appear in perturbation theory when two massless partons become collinear. This part of the method is quite simple and easy to understand. The treatment of the divergences that appear when a gluon becomes soft is a bit more technical and will be given in this paper.

We find that it is conceptually simplest to match showers to a NLO calculation if the NLO calculation is performed in the Coulomb gauge. That is because the collinear divergences of the theory in a physical gauge like the Coulomb gauge are isolated in the cut and virtual self-energy diagrams (just the diagrams that you would draw to illustrate a parton splitting to two partons). Accordingly, the present research program was initiated in Ref. [2], which shows how to do NLO calculations in the Coulomb gauge. I should point out that, although there is a certain conceptual simplicity that emerges through the use of a physical gauge, one can use any gauge, as the recent work of Frixione, Nason, and Webber on the same subject demonstrates [3, 4].

I begin with a brief restatement of the problem. Consider the calculation of an experimental observable that describes a hard scattering process involving strongly interacting particles and suppose that the chosen observable is infrared safe, which makes a perturbative calculation for the observable sensible. The simplest sort of calculation for this purpose consists of calculating the hard process cross section at the lowest order in α_s , call it σ_s^B , at which it occurs. However, one often performs a next-to-leading order calculation, including terms proportional to α_s^B and α_s^{B+1} . Then the estimated error from yet higher order terms (which are usually unknown) is typically smaller than with a leading order calculation.

The NLO calculations are typically in the form of computer programs that act as Monte Carlo generators of partonic events. They produce simulated events with final states consisting of a few partons with specified momenta. For example, for three jet production in electron-positron annihilation, there are three or four partons in the final state. Each event comes with a weight w_n . Then the predicted value for an observable described by a measurement function $S(f)$ is

$$I = \lim_{N \rightarrow \infty} \frac{1}{N} \sum_{n=1}^N w_n S(f_n) \quad (1)$$

A serious weakness of most current NLO Monte Carlo generators is that they produce simulated final states that are not close to physical final states. This contrasts sharply with the highly successful leading order Monte Carlo event generators such as Pythia, Herwig, and Ariadne [5-7], which do generate realistic final states. What could be done to generate realistic final states in an NLO calculation? One might think of using the three and four parton final states in the NLO partonic generators to generate a parton shower from each outgoing parton. This gives a final state with lots of partons. Then one could use one of the leading order Monte Carlo event generators to turn the many partons into hadrons. There should not be a serious problem with the hadronization stage, since this is modelled as a long distance process that leaves infrared safe observables largely unchanged. The problem lies with the parton showers. Here a high energy parton splits into two daughter partons, which

each split into two more partons. As this process continues, the virtualities of successive pairs of daughter partons gets smaller and smaller, representing splittings that happen at larger and larger distance scales. The late splittings leave infrared safe observables largely unchanged. However, the first splittings in a parton shower can involve large virtualities. They represent a mixture of long distance and short distance physics. Thus one must be careful that the showering does not reproduce some piece of short distance physics that was already included in the NLO calculation. To be a little more precise, if one expands the prediction of the calculation including showers in a power series in $\alpha_s(P)$, where P is the hard process scale, in the form

$$I = C_0 \frac{\alpha_s^B}{s} + C_1 \frac{\alpha_s^{B+1}}{s} + C_3 \frac{\alpha_s^{B+2}}{s} + \dots ; \quad (2)$$

then our goal is to insure that the coefficients C_0 and C_1 are exactly the same in the calculation with showers as in the purely perturbative NLO calculation.

The algorithms that we propose apply to showers from final state massless partons. They are illustrated using the process $e^+ + e^- \rightarrow 3$ jets in quantum chromodynamics.¹ While our research program was underway, Frixione and Webber succeeded in matching showers to a NLO calculation for a problem with massless partons in the initial state (but no observed colored partons in the final state) [3]. Subsequently, Frixione, Webber, and Nason have extended this method to a problem with massive colored partons in the final state [4]. Their method is similar to the method presented in Ref. [1], or more precisely to a variant of that method in which the first level of parton splitting, based on Coulomb gauge splitting functions in Ref. [1], is instead based on the splitting functions of Herwig. The soft gluon effects treated in this paper are not part of the algorithms of [3, 4]. Instead, these references employ what amounts to a soft gluon cutoff.² There has been other work on this problem [8]. That of Collins [9] is particularly instructive.

II. THE PROBLEM OF THE SOFT SINGULARITIES

In this section, I describe the particular problem left over from Ref. [1] that remains to be addressed in this paper, recalling just enough of the argument of Ref. [1] to set up the issue.

Consider one of the Born graphs for $e^+ + e^- \rightarrow 3$ jets. Three partons emerge into the final state. The idea presented in Ref. [1] is to let each of these partons split into a pair of partons, as illustrated in Fig. 1. Two features of the splitting are important. First, when the virtuality q^2 of the pair is small, the splitting probability is proportional to $\int P(x) \alpha_s(q^2) dx$ where x is the share of the momentum carried by one of the daughter partons and $P(x)$ is the appropriate Altarelli-Parisi splitting function. Second, the collinear singularity at $q^2 \rightarrow 0$ is damped by a Sudakov factor with the behavior $\exp(-\alpha_s \log^2(q^2))$ for $q^2 \rightarrow 0$. Thus each of the three partons makes a jet, but in the limit of small α_s , each jet is usually very narrow and appears in an infrared safe measurement like a single massless parton. There is a qualifying adverb "usually" here. A fraction α_s of the time, one of the splittings has a

¹ I discuss $e^+ + e^- \rightarrow 3$ jets but not $e^+ + e^- \rightarrow 2$ jets. Thus the present calculation is to be applied with a measurement function that give zero for events that are close to the two jet conformation.

² The parameter C_1 above is then modified by an amount proportional to a positive power of the cutoff parameter δ , so as long as δ is chosen small enough, the cutoff effects in [3, 4] are negligible.

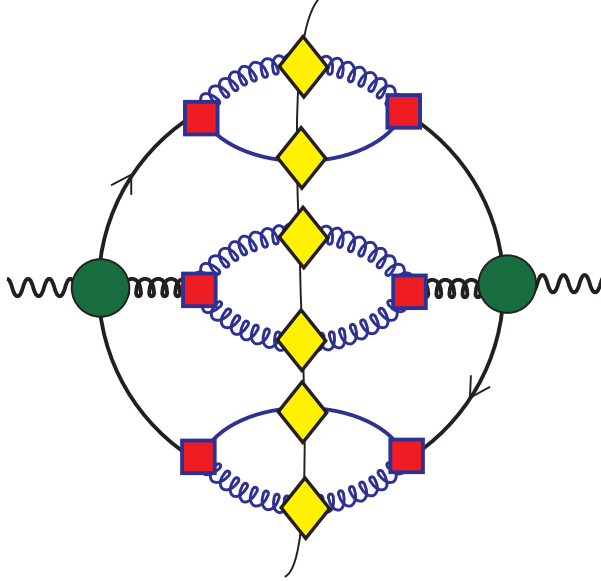


FIG. 1: Primary parton splitting from Ref. [1]. The filled circles represent graphs for the Born amplitude and complex conjugate amplitude. Each of the partons emerging from the Born amplitude splits into two partons with a vertex, represented by the squares, that includes a Sudakov suppression factor. Each of the six daughter partons undergoes further, secondary, splittings and enters the final state as a complete shower. The secondary splittings are represented by the diamonds.

substantial virtuality and we get a four jet final state. Thus there is an order α_s^{B+1} effect in which some probability is removed from the three jet final state and given to a four jet final state. In a purely NLO calculation, this effect is included in the α_s^{B+1} graphs. Thus, to keep the calculation correct to NLO, we subtract these probabilities from the α_s^{B+1} perturbative graphs.

The subtractions are required for NLO consistency of the calculation, but they have another important effect. Since the splitting functions have just the structure found in the order α_s^{B+1} graphs in the collinear limit, the subtractions cancel the collinear singularities (and the collinear soft singularities) of the order α_s^{B+1} graphs. The real and virtual singularities are separately cancelled, whereas without the subtractions the real and virtual singularities are left to cancel against each other (which, of course, they do³). If there were no other singularities, we could let the three and four parton final states of the order α_s^{B+1} graphs develop into parton showers, which would affect the result of the calculation only at order α_s^{B+2} . The calculation would be numerically stable because the integrals for the three and four parton states would be separately finite.

But, of course, there are other singularities, namely the singularities from emission of soft gluons at wide angles from the three hard partons, as well as the corresponding singularities in the α_s^{B+1} virtual graphs. These singularities cancel between the order α_s^{B+1} graphs with

³ We employ a calculation [10{12] in which the integrals over the three-momenta in virtual loops are performed numerically. Then this cancellation happens automatically point by point in the integration. In other methods, the virtual integrals are performed entirely analytically. In this case, the cancellation mechanism is less simple.

three and four final state partons, but we cannot let these two kinds of final states develop separately into showers without losing this cancellation and thus encountering numerical instability.

This is not just a technical problem to be somehow sidestepped. The emission of a soft gluon at order α_s^{B+1} is a real physical effect. It is an effect that does not fit a picture of separate evolution of the three jets because the soft gluon is sensitive to the whole final state. That is, the probability to emit a soft gluon does not break up into the sum of three independent probabilities, one for emission from each jet.

There is a natural way to deal with this. We can consider the three jets to form an antenna that radiates a soft gluon. The radiation probability is proportional to $(f(\theta; \phi) = E) dE d\theta d\phi$, where E is the energy of the gluon, $\theta; \phi$ are its angles, and $f(\theta; \phi)$ is a function that is determined by the directions of the three jets. We can account for the normalization of the radiation probability provided by the virtual graphs by providing a suppression factor with the behavior $\exp(-\alpha_s c_j \log(E))$ for $E \rightarrow 0$. This is depicted in Fig. 2. Thus a soft gluon is always emitted, but when α_s is small the gluon is usually too soft to matter to an infrared safe measurement. However, a fraction α_s of the time the gluon can have a substantial energy and we get a four jet final state. Thus there is an order α_s^{B+1} effect in which some probability is removed from the three jet final state and given to a four jet final state. In the purely NLO calculation, this effect is included in the α_s^{B+1} graphs. Thus, to keep the calculation correct to NLO, we subtract these probabilities from the α_s^{B+1} perturbative graphs.⁴ Of course, the required subtraction terms will be just the soft singularity subtractions that we needed to stabilize the α_s^{B+1} contributions if we add showers separately to α_s^{B+1} graphs with three and four jet final states.

Does the necessity to add soft radiation from a three-jet antenna mean that the standard parton shower Monte Carlo programs such as Herwig, Pythia, and Ariadne need to be rewritten in order to be compatible with an NLO calculation? Not at all. We don't need soft radiation with its correct angular dependence at every stage of a parton shower. All that we need is to radiate one soft gluon from the hard event with its correct angular dependence. This radiation, along with the initial splittings of the three hard partons, can be considered to be part of the NLO calculation, so that the Monte Carlo programs do not need any modification at all. I will add more comments on this subject in the conclusions section of this paper.

III. SOFT GLUON EMISSION

In Ref. [1], we saw that one can turn $\alpha_s [1 + \text{real}(\text{virtual})]$ into $\alpha_s \text{real} \exp(\text{virtual})$ with respect to self-energy graphs, which contain the collinear and collinear soft singularities in the Coulomb gauge. In this section, we begin a detailed description of the singularities generated by the emission of soft gluons at wide angles to the outgoing partons. Up to now in our description, these singularities cancel between real and virtual emissions in the form $\alpha_s [1 + \text{real}(\text{virtual})]$. In the following sections, we turn this into the form $\alpha_s \text{real} \exp(\text{virtual})$ together with some left over nonsingular terms.

⁴ As we shall see, some of the adjustment is to be made in the wide angle part of the splitting functions used to generate the splittings of the three hard partons.

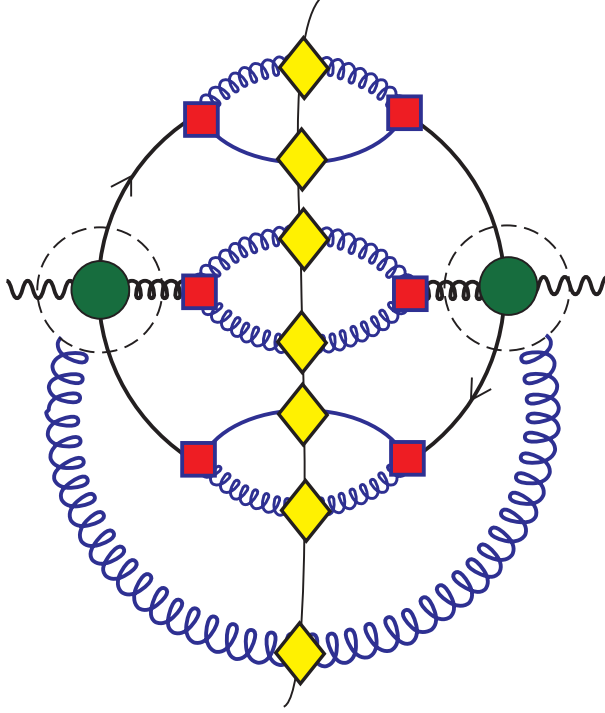


FIG .2: Primary parton splitting with soft gluon radiation added. The graphical symbols of Fig. 1 are also used here. The extra gluon coming from the circles on the right and left represents the soft gluon radiated from the three jets. As with the other partons, the soft gluon undergoes secondary splittings and generates a shower, represented by the diamonds.

Consider a cut Born graph in which the final state has a quark (momentum q_1), a gluon (momentum q_2) and an antiquark (momentum q_3). These partons will make collinear showers, but we ignore that for now. What concerns us here is that these outgoing partons act as an antenna that radiates soft gluons. Let a soft gluon with momentum l be emitted by parton i and, in the complex conjugate amplitude, absorbed by parton j .

We need to specify the kinematics in a definite way. We choose to route the momenta for the $fi; jg$ term so that the momenta $p_1^{(ij)}; p_2^{(ij)}; p_3^{(ij)}$ carried by, respectively, the quark, the gluon, and the antiquark in the final state are given by

$$p_k^{(ij)} = q_k - \frac{1}{2} (k_i + k_j)l \quad (3)$$

Thus for a graph with $i = j$, the momentum k before the soft gluon emission is $\tilde{k} = q$ and afterwards it is $p = q - l$. For a graph with $i \neq j$, the momentum k before the soft gluon emission is $\tilde{k} = q + \frac{1}{2}l$ and afterwards it is $p = q - \frac{1}{2}l$.

A . The soft gluon approximation

We now specify the approximation to be applied for the soft gluon emission [13]. Let a parton with momentum k emit a soft gluon with momentum l and enter the final state with momentum p . Then $l = k - p$. The momenta p and k are approximately in the direction

of a light-like vector u . We take $u = (1; \hat{q})$ where $\hat{q} = \hat{q}_i - \hat{q}_j$ and q is $\frac{1}{2}(k + p)$ in the case of an $i \leftrightarrow j$ graph or k in the case of an $i = j$ graph, as specified in Eq. (3).

The approximation is based on the fact that the soft gluon sees a current J that is approximately proportional to u . Thus if we denote the polarization vector of the gluon by ϵ , we can replace

$$J \cdot \epsilon \approx J \cdot \frac{u}{u \cdot \epsilon} \epsilon \quad (4)$$

This replacement becomes exact in the limit in which J approaches u for some constant ϵ . It is important that the momentum l not point along u . That is, the gluon momentum should be small so that both k and p and thus J are approximately proportional to u , but the gluon momentum should not be collinear with the momentum of the emitting parton.

For the graph in which the soft gluon goes from parton i to parton j , the factors $u_i = u_j = u$, together with appropriate color matrices, give a factor (in the Coulomb gauge)

$$C_{ij} \frac{u_i \cdot u_j D(l)}{(u_i \cdot l)(u_j \cdot l)} = \frac{C_{ij}}{\Upsilon^2} \frac{(\hat{q}_i \cdot \hat{q}_j)(\hat{l} \cdot \hat{q})(\hat{l} \cdot \hat{q})}{(1 - \hat{l} \cdot \hat{q})(1 - \hat{l} \cdot \hat{q})} \quad (5)$$

Here $D(l)$ is the Coulomb gauge numerator factor

$$D(l) = g + \frac{1}{\Upsilon^2} l \cdot \Upsilon \Upsilon \cdot l + l \cdot l^i \quad (6)$$

where Υ is $(0; \Upsilon^1; \Upsilon^2; \Upsilon^3)$. The constants C_{ij} are the color factors for this process,

$$\begin{aligned} C_{12} = C_{21} = C_{23} = C_{32} &= \frac{N_c}{2}; \\ C_{13} = C_{31} &= \frac{1}{2N_c}; \\ C_{11} = C_{33} &= C_F; \\ C_{22} &= C_A; \end{aligned} \quad (7)$$

What about the factor $J \cdot l$? In the case of emission from a quark, we have (since $\hat{p} = 0$)

$$\not{p} \cdot k \not{p} \frac{k}{k^2} = \not{p}; \quad (8)$$

so we simply include a factor \not{p} for the final state quark. The final state phase space associated with the original graph has a factor $1 = (2\pi)^3$. We retain this factor without change.

For emission from an antiquark we have [noting that the momenta p and q are directed against the fermion number flow and that we should extract a factor (-1) to associate with the color factor for the graph]

$$(-1) \frac{(\not{k})}{k^2} (\not{k} \not{p}) (\not{p}) = \not{p}; \quad (9)$$

so we simply include a factor \not{p} for the final state antiquark. The final state phase space associated with the original graph has a factor $1 = (2\pi)^3$. We retain this factor without change.

The case of emission from a gluon is a bit more complicated. We denote the tensor associated with the vertex function by

$$V(k_A; k_B; k_C) = g(k_A, k_B) + \text{cyclic permutations} \quad (10)$$

Then the three gluon vertex function with momenta $k_A; k_B; k_C$ directed into the vertex is $(ig)(if_{abc})V(k_A; k_B; k_C)$: The vertex dotted into (k, p) times the adjoining propagator and the propagator numerator for the final state gluon, with the ig and the color matrix if_{abc} removed, is

$$\begin{aligned} D(p) V^h(p; k; p-k)(k, p) &= \frac{i D(k)}{k^2} \\ &= D(p) (k^2 g - k k) (p^2 g - p p) \frac{i D(k)}{k^2} \\ &= D(p) (k^2 g - k k) \frac{D(k)}{k^2} \\ &= D(p) \left(g + \frac{1}{k^2} k k \right) \\ &= D(p) \left(g + \frac{1}{k^2} (p + \Gamma) k \right) \\ &= D(p) \left(g + \frac{1}{k^2} \Gamma k \right) \\ &= D(p) : \end{aligned} \quad (11)$$

Here in the second to last step we have noted that $D(p) p = 0$. Then in the last step we drop the term proportional to 1 so as to simplify our soft gluon approximation. Thus the net result of the approximation is to include, in addition to the factor $u = u_1$, a factor $D(p)$ for the final state gluon. The final state phase space associated with the original graph has a factor $1 = (2\pi)^3$. We retain this factor without change.

It is important that the factors in Eqs. (8), (9) and (11) revert to the factors in the Born diagram when $\Gamma \rightarrow 0$.

B. The added terms

We can now apply these ideas. We write the contribution to the cross section from a given cut Born level graph as

$$\begin{aligned} I[\text{Born}] &= \int_{\mathcal{Q}_1}^Z \int_{\mathcal{Q}_2}^Z \int_{\mathcal{Q}_3}^Z \int_{\mathcal{Q}_4}^X G_3(\mathcal{Q}_1; \mathcal{Q}_2; \mathcal{Q}_3) \\ & f_3(\mathcal{Q}_1; \mathcal{Q}_2; \mathcal{Q}_3) S_3(\mathcal{Q}_1; \mathcal{Q}_2; \mathcal{Q}_3) : \end{aligned} \quad (12)$$

Here S_3 is the final state measurement function (see Eq. (4) of Ref. [1]) and f_3 contains the factors from the Feynman rules corresponding to the three final state particles, which, suppressing the Dirac and Lorentz indices, are

$$f_3(\mathcal{Q}_1; \mathcal{Q}_2; \mathcal{Q}_3) = \frac{\not{\mathcal{Q}}_1}{2\mathcal{J}_1} \frac{D(\mathcal{Q}_2)}{2\mathcal{J}_2} \frac{\not{\mathcal{Q}}_3}{2\mathcal{J}_3} : \quad (13)$$

The function G_3 contains everything else, including an amputated Green function times a hermitian conjugate amputated Green function. With this notation, we write the terms to be added for real soft gluon emission as

$$\begin{aligned} I[\text{soft}; \text{real}] &= \int d\epsilon_1 \int d\epsilon_2 \int d\epsilon_3 \int \mathbb{1} G_3(\epsilon_1; \epsilon_2; \epsilon_3) \\ &= \frac{g_s^2}{(2\pi)^3} \int \frac{d\mathbb{1}}{2\mathbb{1}j} \frac{1}{\mathbb{1}^2} \Theta(\mathbb{1}^2 < M_{\text{soft}}^2) \int_{ij} F_{ij}(\hat{\mathbb{1}}; \hat{\epsilon}_1; \hat{\epsilon}_2; \hat{\epsilon}_3) \\ &= f_3(\mathbf{p}_1^{(ij)}; \mathbf{p}_2^{(ij)}; \mathbf{p}_3^{(ij)}) S_4(\mathbf{p}_1^{(ij)}; \mathbf{p}_2^{(ij)}; \mathbf{p}_3^{(ij)}; \mathbb{1}); \end{aligned} \quad (14)$$

where $\mathbf{p}_k^{(ij)}$ are defined in Eq. (3) and S_4 is the measurement function for four final state particles.

The factor $\Theta(\mathbb{1}^2 < M_{\text{soft}}^2)$ is inserted to suppress contributions from momenta $\mathbb{1}$ that are outside the range of validity of the soft gluon approximation. We take

$$M_{\text{soft}} = \frac{P_{\text{soft}}}{s_0} (1 - t_0); \quad (15)$$

where $\frac{P_{\text{soft}}}{s_0}$ and t_0 are, respectively, the cm. energy and the thrust of the final state with parton momenta $\epsilon_1; \epsilon_2; \epsilon_3$ and where we take the parameter $\frac{P_{\text{soft}}}{s_0}$ to be $1/3$.

The functions F_{ij} are, for $i \neq j$,

$$F_{ij} = C_{ij} \frac{\hat{\epsilon}_i \cdot \hat{\epsilon}_j (\hat{\mathbb{1}} \cdot \hat{\epsilon}_i \hat{\mathbb{1}} \cdot \hat{\epsilon}_j)}{(1 - \hat{\mathbb{1}} \cdot \hat{\epsilon}_i)(1 - \hat{\mathbb{1}} \cdot \hat{\epsilon}_j)}; \quad (16)$$

as specified in Eq. (5). For $i = j$ we begin with a factor

$$C_{ii} \frac{1 + \hat{\mathbb{1}} \cdot \hat{\epsilon}_i}{(1 - \hat{\mathbb{1}} \cdot \hat{\epsilon}_i)^2} = C_{ii} \frac{1 + \hat{\mathbb{1}} \cdot \hat{\epsilon}_i}{1 - \hat{\mathbb{1}} \cdot \hat{\epsilon}_i}; \quad (17)$$

We use Eq. (7) to break C_{ii} up into

$$C_{ii} = \sum_{\substack{a=1 \\ a \neq i}}^3 C_{ia}; \quad (18)$$

Then in the term proportional to C_{ia} , we impose the condition that the angle between $\mathbb{1}$ and ϵ_i should be greater than the angle between ϵ_a and ϵ_i . That is, our soft gluon for $i = j$ should be soft but not collinear, and we impose a cut to enforce that condition. Thus we take

$$F_{ii} = \frac{1 + \hat{\mathbb{1}} \cdot \hat{\epsilon}_i}{1 - \hat{\mathbb{1}} \cdot \hat{\epsilon}_i} \left(\sum_{\substack{a=1 \\ a \neq i}}^3 C_{ia} \Theta(\hat{\mathbb{1}} \cdot \hat{\epsilon}_i > \hat{\epsilon}_a \cdot \hat{\epsilon}_i) \right); \quad (19)$$

It will be useful to have at hand an abbreviated notation based on the definitions

$$R_0(\epsilon_1; \epsilon_2; \epsilon_3) = G_3(\epsilon_1; \epsilon_2; \epsilon_3) f_3(\epsilon_1; \epsilon_2; \epsilon_3) S_3(\epsilon_1; \epsilon_2; \epsilon_3) \quad (20)$$

and

$$R_{ij}(\mathbb{1}; \epsilon_1; \epsilon_2; \epsilon_3) = G_3(\epsilon_1; \epsilon_2; \epsilon_3) f_3(\mathbf{p}_1^{(ij)}; \mathbf{p}_2^{(ij)}; \mathbf{p}_3^{(ij)}) S_4(\mathbf{p}_1^{(ij)}; \mathbf{p}_2^{(ij)}; \mathbf{p}_3^{(ij)}; \mathbb{1}); \quad (21)$$

With this notation, the Born and soft-real contributions are

$$I[\text{Born}] = \int d\epsilon_1 \int d\epsilon_2 \int d\epsilon_3 \int \epsilon_i R_0(\epsilon_1; \epsilon_2; \epsilon_3) \quad (22)$$

and

$$I[\text{soft}; \text{real}] = \int d\epsilon_1 \int d\epsilon_2 \int d\epsilon_3 \int \epsilon_i \int_0^{M_{\text{soft}}} \frac{d\hat{\Gamma}_j}{\hat{\Gamma}_j} \int \frac{d^2 \hat{\Gamma}}{4} \int_{ij}^s F_{ij}(\hat{\Gamma}; \hat{q}_1; \hat{q}_2; \hat{q}_3) R_{ij}(\Gamma; \epsilon_1; \epsilon_2; \epsilon_3): \quad (23)$$

The indicated integration over $\hat{\Gamma}$ is an integration over the unit sphere.

We define a corresponding virtual soft gluon contribution that will cancel the real soft gluon contribution for small Γ as long as the measurement function is infrared safe, so that $R_{ij} \neq R_0$ for $\Gamma \neq 0$:

$$I[\text{soft}; \text{virtual}] = \int d\epsilon_1 \int d\epsilon_2 \int d\epsilon_3 \int \epsilon_i \int_0^{M_{\text{soft}}} \frac{d\hat{\Gamma}_j}{\hat{\Gamma}_j} \int \frac{d^2 \hat{\Gamma}}{4} \int_{ij}^s F_{ij}(\hat{\Gamma}; \hat{q}_1; \hat{q}_2; \hat{q}_3) R_0(\epsilon_1; \epsilon_2; \epsilon_3): \quad (24)$$

Conveniently, the integral over the angles of $\hat{\Gamma}$ in $I[\text{soft}; \text{virtual}]$ is simple:

$$\begin{aligned} \int \frac{d^2 \hat{\Gamma}}{4} \int_{ij}^s F_{ij}(\hat{\Gamma}; \hat{q}_1; \hat{q}_2; \hat{q}_3) &= \int_{i=1}^2 \int_{j=i+1}^3 (C_{ij}) (1 - \hat{q}_i \cdot \hat{q}_j) \\ &= \frac{N_C}{2} [(1 - \hat{q}_1 \cdot \hat{q}_2) + (1 - \hat{q}_2 \cdot \hat{q}_3)] \frac{1}{2N_C} (1 - \hat{q}_1 \cdot \hat{q}_3): \end{aligned} \quad (25)$$

The integral is largest when $\hat{q}_i \cdot \hat{q}_j = 1$, which implies $\hat{q}_1 \cdot \hat{q}_2 = \hat{q}_2 \cdot \hat{q}_3 = 1$. Then the integral is $2N_C = 2C_A$. The integral is smallest when $\hat{q}_1 \cdot \hat{q}_2 = 1$, or else $\hat{q}_2 \cdot \hat{q}_3 = 1$. Then the integral is $N_C = 1/2 N_C = 2C_F$.

We will, in due course, see how to exponentiate the added contributions $I[\text{soft}; \text{real}] + I[\text{soft}; \text{virtual}]$. First, however, we must subtract these terms from I so that the cross section remains unchanged.

IV. ADJUSTING THE COLLINEAR TERMS

The terms in Eqs. (23) with $i = j$ represent soft gluon approximations to the cut self-energy diagrams for outgoing partons i . Thus we should subtract them from the exact cut self-energy diagrams. Consider, for example, $i = j = 1$, corresponding to a self-energy insertion on the outgoing quark propagator. This contribution has the form given in Eq. (7) of Ref. [1],

$$I[\text{real}] = \int \frac{d\epsilon_1}{2\hat{\Gamma}_1} \text{Tr} \left(\int_0^{Z_1} \frac{dq^2}{q^2} \int_0^{Z_1} dx \frac{d}{2} \frac{s}{2} M_{g=q}(q^2; x;) R(q^2; x;) \right); \quad (26)$$

where $q = q_1$ and the notation, including the variables $(q^2; x;)$, is explained in Sec. III of Ref. [1]. We can translate the $f_{1;1j}$ term in Eq. (23) into the notation used in this equation by using the change of variable

$$\frac{dI}{2\pi j} = \frac{1}{8\pi j} \int_0^z dq^2 \int_0^z dx \frac{1}{1+} ; \quad (27)$$

where

$$1+ = \frac{q}{1+q^2=q^2}; \quad (28)$$

Then

$$I_{11}[\text{soft}; \text{real}] = \frac{dq}{2\pi j} \text{Tr} \left(\int_0^z \frac{dq^2}{q^2} \int_0^z dx \frac{d}{2} \frac{1}{1+} \frac{q^2}{\Gamma^2 4} \right) \quad (\Gamma^2 < M_{\text{soft}}^2)$$

$$\frac{1+\hat{q}}{1-\hat{q}} \left(1 \right) C_{1a} \hat{q} < \hat{q} \quad \hat{q} \quad \hat{q} \quad \hat{q} \quad \Delta R(q^2; x;) : \quad (29)$$

$\frac{a=1}{a \neq 1}$

Now we can use

$$\Gamma^2 = \frac{q^2}{4} (+ 2x)^2$$

$$q^2 = q^2 (2+)$$

$$\hat{q} = \frac{2x + 2x}{+ 2x} \quad (30)$$

to rewrite this as

$$I_{11}[\text{soft}; \text{real}] = \frac{dq}{2\pi j} \text{Tr} \left(\int_0^z \frac{dq^2}{q^2} \int_0^z dx \frac{d}{2} \frac{1}{1+} (+ 2x < 2M_{\text{soft}} = \pi j) \right)$$

$$\left(1 \right) C_{1a} \frac{2x + 2x}{+ 2x} < \hat{q} \quad \hat{q}$$

$\frac{a=1}{a \neq 1}$

$$\frac{s}{2} \frac{8x}{(+ 2x)^2} \frac{(1+ =2)^2}{1-x} \quad \Delta R(q^2; x;) : \quad (31)$$

Thus we can subtract $I_{11}[\text{soft}; \text{real}]$ by replacing $M_{g=q}(q^2; x;)$ by

$$M_{g=q}(q^2; x;) \quad \Delta P_1^{\text{soft}}(q^2; x;) \quad (32)$$

where

$$P_1^{\text{soft}}(q^2; x) = (+ 2x < 2M_{\text{soft}} = \pi j) \left(1 \right) C_{ia} \frac{2x + 2x}{+ 2x} < \hat{q} \quad \hat{q}$$

$\frac{a=1}{a \neq 1}$

$$\frac{8x}{1-x} \frac{1}{(+ 2x)^2} \frac{(1+ =2)^2}{1+} : \quad (33)$$

The effect of this is to remove the part of M that is singular when $j_{1j} \neq 0$ at a fixed angle greater than the angle between the quark and the other two outgoing partons. Note that $j_{1j} \neq 0$ at a fixed angle corresponds to $\neq 0$ and $x \neq 0$ with $=x$ fixed.

The term in Eq. (23) for emission from the antiquark line, $I_{33}[\text{soft};\text{real}]$ is given by Eq. (31) with $(\not{q} - \not{\Lambda})$ replaced by $(\not{q} + \not{\Lambda})$ and the index 1 replaced by 3. Thus we can subtract $I_{33}[\text{soft};\text{real}]$ by replacing $M_{g=q}(\not{q}^2; \mathbf{x}; \cdot)$ in the analogue of Eq. (26) by

$$M_{g=q}(\not{q}^2; \mathbf{x}; \cdot) = (\not{q} + \not{\Lambda}) P_3^{\text{soft}}(\not{q}^2; \mathbf{x}); \quad (34)$$

with the function $P_3^{\text{soft}}(\not{q}^2; \mathbf{x})$ given in Eq. (33) with $i = 3$.

Finally, the term in Eq. (23) for emission from the gluon line, $I_{22}[\text{soft};\text{real}]$ is given by

$$I_{22}[\text{soft};\text{real}] = \int_0^Z \frac{d\eta}{2\eta} \int_0^Z \frac{dq^2}{q^2} \int_0^Z dx \frac{d}{2} \frac{s}{2} P_2^{\text{soft}}(\not{q}^2; \mathbf{x}) D(\not{q} - \not{\Lambda}) R(\not{q}^2; \mathbf{x}); \quad (35)$$

with the function $P_2^{\text{soft}}(\not{q}^2; \mathbf{x})$ given in Eq. (33) with $i = 2$. Thus we can subtract $I_{22}[\text{soft};\text{real}]$ by replacing $M_{g=g}(\not{q}^2; \mathbf{x}; \cdot)$ in the analogue of Eq. (26) by

$$M_{g=g}(\not{q}^2; \mathbf{x}; \cdot) = D(\not{q} - \not{\Lambda}) P_2^{\text{soft}}(\not{q}^2; \mathbf{x}); \quad (36)$$

[There is also a $g \rightarrow qq$ splitting function $M_{g=q}$, but there is no soft singularity for $g \rightarrow qq$ so this function does not get modified.]

The terms in Eq. (24) with $i = j$ represent soft gluon approximations to the virtual self-energy diagrams for outgoing partons i . Thus we should subtract them from the exact virtual self-energy diagrams. Consider the virtual self-energy insertion on the outgoing quark propagator. This contribution has the form given in Eq. (12) of Ref. [1],

$$I[\text{virtual}] = \int_0^Z \frac{d\eta}{2\eta} \text{Tr} \left(\int_0^Z \frac{dq^2}{q^2} \int_0^Z dx \frac{d}{2} \frac{s}{2} P_{g=q}(\not{q}^2; \mathbf{x}) \not{q} R_0 \right); \quad (37)$$

The functions $P_{a \rightarrow b}$ are given in the Appendix of Ref. [1]. When translated into the notation used in this equation, the $fl;lg$ term in Eq. (24) is

$$I_{11}[\text{soft};\text{virtual}] = \int_0^Z \frac{d\eta}{2\eta} \text{Tr} \left(\int_0^Z \frac{dq^2}{q^2} \int_0^Z dx \frac{d}{2} \frac{s}{2} P_1^{\text{soft}}(\not{q}^2; \mathbf{x}) \not{q} R_0 \right); \quad (38)$$

where P_1^{soft} is defined in Eq. (33). Thus we can subtract $I_{11}[\text{soft};\text{virtual}]$ by replacing $P_{g=q}(\not{q}^2; \mathbf{x})$ by

$$P_{g=q}(\not{q}^2; \mathbf{x}) = P_1^{\text{soft}}(\not{q}^2; \mathbf{x}); \quad (39)$$

Similarly, we can subtract $I_{33}[\text{soft};\text{virtual}]$ by replacing $P_{g=q}(\not{q}^2; \mathbf{x}) = P_{g=q}(\not{q}^2; \mathbf{x})$ in the analogue of Eq. (37) by

$$P_{g=q}(\not{q}^2; \mathbf{x}) = P_3^{\text{soft}}(\not{q}^2; \mathbf{x}) \quad (40)$$

and we can subtract $I_{22}[\text{soft};\text{virtual}]$ by replacing $P_{g=g}(\not{q}^2; \mathbf{x})$ in the analogue of Eq. (37) by

$$P_{g=g}(\not{q}^2; \mathbf{x}) = P_2^{\text{soft}}(\not{q}^2; \mathbf{x}); \quad (41)$$

After the collinear splitting terms have been adjusted to remove their wide angle soft parts, we turn $\backslash\text{Bom}[\text{real} + \text{virtual}]\text{"}$ for the collinear splittings into $\backslash\text{Bom}[\text{real} \exp(\text{virtual})]\text{"}$ as explained in Ref. [1]. The only difference is that the meaning of $\backslash\text{real}\text{"}$ and $\backslash\text{virtual}\text{"}$ here have been slightly changed.

V. ADJUSTING THE NLO GRAPHS

It remains to subtract the terms $I_{ij}[\text{soft};\text{real}]$ and $I_{ij}[\text{soft};\text{virtual}]$ for $i \notin j$ from I . Recall that we include in the calculation the cut order $\frac{B+1}{s}$ graphs that do not have a cut self-energy subdiagram or a virtual self-energy subdiagram with the immediately adjacent propagator cut. [We also include diagrams with cut self-energy subdiagrams, but with a theta function that requires the virtuality in the self-energy subdiagram to be large.] The included graphs have soft gluon divergences, which cancel between real and virtual soft gluon emissions. We will subtract the approximate soft gluon contributions from these exact contributions, so that the soft gluon divergences are cancelled separately for the real and virtual contributions.

A. Real soft gluons

This is simple for the real emission terms, $I[\text{soft};\text{real}]$. Consider a cut order $\frac{B+1}{s}$ graph with four parton lines cut. The cut lines are a quark and an antiquark plus either two gluons or another quark and antiquark. In the case of a quark and an antiquark plus another quark and antiquark, we do nothing. In the case of a quark and an antiquark plus two gluons, we designate one of the gluons as potentially soft. Then this cut graph corresponds to the contribution from one of the possible Born graphs to one of the terms in $I[\text{soft};\text{real}]$, which has two gluons in the final state, one of them "hard" and one soft. We simply subtract this contribution to $I[\text{soft};\text{real}]$ from the cut graph in question. Now we designate the other final state gluon as potentially soft, and the corresponding contribution to $I[\text{soft};\text{real}]$ and subtract it.

This procedure has two effects. First, we use up all of the terms in $I[\text{soft};\text{real}]$ that we needed to subtract from I . Second, the cut next-to-leading order graph with these counterterms has only integrable soft-gluon singularities since the singularities of the counterterms match the singularities of the cut order $\frac{B+1}{s}$ graph when either of the gluons become soft. Furthermore, the cancelling terms have the same final states: we are cancelling graphs with four final state partons against counterterms with the same four final state partons.

B. Virtual soft gluons

Subtracting the virtual terms, $I[\text{soft};\text{virtual}]$ requires a bit more analysis. We want to subtract these terms from the cut next-to-leading order graphs with three partons in the final state { a quark, a gluon, and an antiquark. Such a cut graph has a virtual loop either to the right of the final state cut or to the left. We want the contributions from

$I[\text{soft};\text{virtual}]$ to cancel the soft gluon singularities from these virtual loops. However, the terms in $I[\text{soft};\text{virtual}]$, as written, do not have the right structure to effect the cancellation. Thus we need to rearrange the terms.

In the $fi;jg$ term in $I[\text{soft};\text{virtual}]$ we have the function

$$F_{ij}(\hat{l}) = C_{ij} \frac{\hat{q}_i \cdot \hat{q} \cdot (\hat{l} \cdot \hat{q} \cdot \hat{q})}{(1 - \hat{l} \cdot \hat{q})(1 - \hat{l} \cdot \hat{q})} \quad (42)$$

In the $fj;ig$ term we choose to redefine the integration variable so that $\hat{l} \rightarrow -\hat{l}$. Then we

with $J = L$ or $J = R$ depending on whether the virtual loop was to the left of the cut or to the right. We do this for each potentially soft gluon in the virtual loop.

This procedure takes care of the terms in I [soft;virtual] that we needed to subtract from I . Additionally, the singularity of the counter term matches the singularity of the graph when either of the gluons become soft (see [11]) so that the graph with these counter-terms has only integrable soft-gluon singularities.

There are some technical issues to attend to. First, one should match the integration variables in the loop graph to the integration variables in the counterterm, so that $q_1; q_2; q_3; q$ are the momenta of the final state partons and l is the momentum of the potentially soft gluon in each case. Second, one needs to deform the integration contour for the counterterm according to the $i\epsilon$ prescriptions indicated. This deformation should closely match that of the next-to-leading order graph in the limit of small l , as discussed in the Appendix.

VI. SECONDARY SHOWERING FROM NLO GRAPHS

We have started with the order α_s^{B+1} graphs simply as specified by the Feynman rules and then, because there are order α_s^{B+1} effects incorporated in the splittings of the partons emerging from the α_s^B graphs and in the soft gluon radiation from the α_s^B graphs, we have subtracted certain quantities from the α_s^{B+1} graphs. The result is that the subtracted α_s^{B+1} graphs with and without virtual loops are separately free of infrared divergences.

One can attach a shower to each final state parton emerging from a subtracted order α_s^{B+1} graph. Each shower affects the expectation value of the observable being calculated. However, according to the argument in Ref. [1], as long as the observable is infrared safe, the effect is to add terms proportional to α_s^{B+2} and higher powers of α_s . This holds independently of the exact functions used to generate the showers, as long as these functions have the required generic properties. For our present purposes, we can use the simple algorithm described in Sec. VIII of Ref. [1].

The only thing that we need to specify is the choice for width parameter for the first splitting in the shower. We will take

$$w^2 = \alpha_s^2 (1 - t); \quad (50)$$

where q is the momentum of the parton that is to split and t is the thrust of the partonic final state in the order α_s^{B+1} graph. The factor $(1 - t)$ is important. In the case that we generate an event with thrust very near to 1, we do not want the showering to turn this two jet event into a three jet event, an event with thrust substantially less than 1. The factor $(1 - t)$ prevents this. (For thrust greater than a value t_{max} close to 1, the code [14] provides a stronger cut: $w^2 = \alpha_s^2 (1 - t)^2 = (1 - t_{max})^2$. The default value of t_{max} is 0.95.)

VII. EXPONENTIATION

We now return to the terms that we have added. Consider the sum

$$I[Bom] + I[soft;real] + I[soft;virtual] \quad (51)$$

from Eqs. (22), (23), and (24). Compare this to the quantity

$$I[\text{radiate}] = \int_{\alpha_1}^Z \int_{\alpha_2}^Z \int_{\alpha_3}^Z \int_{\alpha_i}^X \int_0^Z M_{\text{soft}} \frac{d\vec{l}_j}{l_j} \frac{d^2\hat{l}}{4}$$

$$\int_{ij}^X \frac{-s}{0} F_{ij}(\hat{L}; \hat{Q}_1; \hat{Q}_2; \hat{Q}_3) R_{ij}(\underline{L}; \underline{Q}_1; \underline{Q}_2; \underline{Q}_3) \exp^{\int_{ij}^Z M_{\text{soft}} \frac{d\hat{L}^0_j}{\hat{L}^0_j} \int_{ij}^Z \frac{d^2 \hat{L}^0}{4} X \frac{-s}{i^0_j} F_{i^0_j}(\hat{L}^0; \hat{Q}_1; \hat{Q}_2; \hat{Q}_3)^A} : \quad (52)$$

Here the three outgoing partons radiate a soft gluon according to the radiation pattern specified by the F_{ij} . The gluon radiation at small \hat{L} is suppressed by the exponential function, which gives the probability that the gluon was not already radiated with a higher energy than \hat{L}_j . As we found in the companion paper [1] on collinear emissions, there is a subtraction to multiplication theorem that says that

$$I[\text{Bom}] + I[\text{soft;real}] + I[\text{soft;virtual}] = I[\text{radiate}] \quad 1 + O\left(\frac{2}{s}\right) : \quad (53)$$

The proof of this is simple. We have

$$I[\text{radiate}] = I[\text{radiate;1}] + I[\text{radiate;2}] ; \quad (54)$$

where

$$I[\text{radiate;1}] = \int_{ij}^X \frac{-s}{0} F_{ij}(\hat{L}; \hat{Q}_1; \hat{Q}_2; \hat{Q}_3) R_{ij}(\underline{L}; \underline{Q}_1; \underline{Q}_2; \underline{Q}_3) R_0(\underline{Q}_1; \underline{Q}_2; \underline{Q}_3) \exp^{\int_{ij}^Z M_{\text{soft}} \frac{d\hat{L}^0_j}{\hat{L}^0_j} \int_{ij}^Z \frac{d^2 \hat{L}^0}{4} X \frac{-s}{i^0_j} F_{i^0_j}(\hat{L}^0; \hat{Q}_1; \hat{Q}_2; \hat{Q}_3)^A} : \quad (55)$$

and

$$I[\text{radiate;2}] = \int_{ij}^X \frac{-s}{0} F_{ij}(\hat{L}; \hat{Q}_1; \hat{Q}_2; \hat{Q}_3) R_0(\underline{Q}_1; \underline{Q}_2; \underline{Q}_3) \exp^{\int_{ij}^Z M_{\text{soft}} \frac{d\hat{L}^0_j}{\hat{L}^0_j} \int_{ij}^Z \frac{d^2 \hat{L}^0}{4} X \frac{-s}{i^0_j} F_{i^0_j}(\hat{L}^0; \hat{Q}_1; \hat{Q}_2; \hat{Q}_3)^A} : \quad (56)$$

Now $I[\text{radiate;1}]$ can be expanded in powers of s to give

$$I[\text{radiate;1}] = \int_{ij}^X \frac{-s}{0} F_{ij}(\hat{L}; \hat{Q}_1; \hat{Q}_2; \hat{Q}_3) R_{ij}(\underline{L}; \underline{Q}_1; \underline{Q}_2; \underline{Q}_3) R_0(\underline{Q}_1; \underline{Q}_2; \underline{Q}_3) + O\left(\frac{2}{s} R\right) : \quad (57)$$

This is just $I[\text{soft;real}] + I[\text{soft;virtual}]$. The integral in $I[\text{radiate;2}]$ looks complicated, but it is simple because the \hat{L}_j integral is the integral of a derivative. Thus $I[\text{radiate;2}]$ is exactly $I[\text{Bom}]$:

$$I[\text{radiate;2}] = \int_{ij}^X \frac{-s}{0} F_{ij}(\hat{L}; \hat{Q}_1; \hat{Q}_2; \hat{Q}_3) R_0(\underline{Q}_1; \underline{Q}_2; \underline{Q}_3) : \quad (58)$$

This proves the theorem .

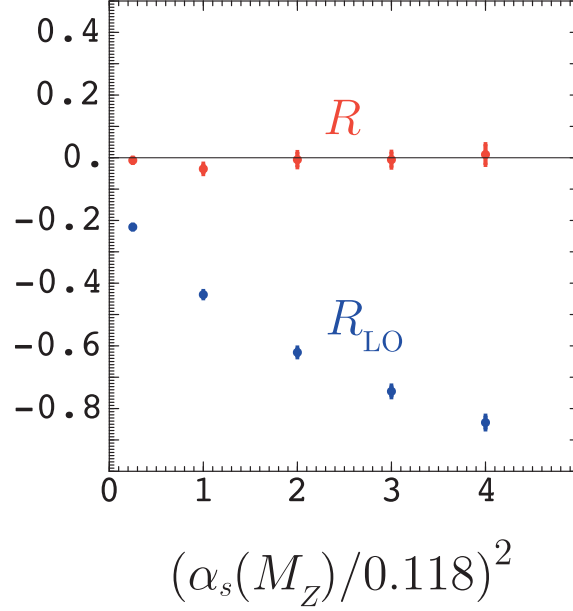


FIG. 3: Comparison of the NLO calculation with showers added as described in this paper and [1] to a pure NLO calculation using [14]. I plot the ratio R defined in Eq. (61) for the thrust distribution at thrust equal 0.86. Also shown is the ratio R_{LO} , defined in Eq. (62), in which the order α_s^{B+1} correction terms are omitted from the calculation. The cm. energy is $\sqrt{s} = M_Z$ and the renormalization scale is chosen to be $\mu = \sqrt{s} = 6$. These ratios are calculated for $\alpha_s(M_Z)^2 = 0.25; 1; 2; 3; 4$ and $(0.118)^2$ and plotted versus $\alpha_s(M_Z)^2 = (0.118)^2$.

coefficient of $[\frac{\alpha_s}{s}]^{l=2}$ in R_{LO} does not have any great significance, since it is quite sensitive to the choice of renormalization scale.

The results of this test are shown in Fig. 3 for $\sqrt{s} = M_Z$ with a renormalization scale $\mu = \sqrt{s} = 6$. The values of $\alpha_s(M_Z)$ range from $(l=2) 0.118$ to $2 \cdot 0.118$, where 0.118 represents something close to the physical value for $\alpha_s(M_Z)$. One should note that $2 \cdot 0.118$ amounts to quite a large α_s in this calculation since $\alpha_s(M_Z) = 0.236$ gives $\alpha_s(\mu) = 0.586$.

We see the expected shape of the R_{LO} curve. We also see that the R curve lies closer to zero, indicating that the α_s^{B+1} corrections are approximately right. A more exacting test is to examine whether the R curve approaches a straight line through the origin as $\frac{\alpha_s}{s} \rightarrow 0$. Within the errors, it does. However, the slope of the straight line is not significantly different from zero. Presumably with other choices of parameters in the program, the absolute value of the slope would be bigger.

X. AREAS WHERE MORE WORK IS NEEDED

The present work suffers from a number of deficiencies. First, the code is designed to calculate three jet cross sections in electron-positron annihilation correctly to NLO, but it ignores the two jet cross section. It should be rather simple to calculate the two jet cross section at next-to-leading order with showers. Then one should merge the two calculations so that three jet observables are calculated correctly at order α_s^2 while the two jet cross section is calculated correctly at order α_s^1 . Second, it is desirable to add not only parton showers

but hadronization to NLO perturbative calculations. For hadronization, one can use an existing model [5,7]. However, most hadronization models require color information on the final state partons. Since the current code does not assign a color structure to these partons, it will be necessary to add this capability. Third, in principle, hadronization models should be infrared safe in the sense that final partonic states that differ by a parton splitting into two almost collinear partons (or one parton and another with almost zero momentum) will produce almost the same hadronic final state. Since hadronization models currently in use do not necessarily have this property, the NLO calculation should provide it by combining parton pairs with virtuality less than some cutoff parameter matched to the hadronization model to be used. Finally, the current paper includes hardly any numerical investigations to check how well the program works for various observables and how the results depend on parameters such as the renormalization scale and the soft gluon limiting energy M_{soft} . Addressing these needs remains a topic for future research.

XI. CONCLUSIONS

In this paper and [1], we have seen how to add parton showers to a next-to-leading order calculation in QCD in such a way that the result obtained for an infrared safe observable remains correct to next-to-leading order. The main feature of this procedure is to turn the collinear singularities of the order \mathcal{B}_s^{B+1} graphs into the primary parton splittings, that is the first splittings of the partons that emerge from an \mathcal{B}_s^B graph. This was accomplished in [1] in a particularly simple fashion by virtue of the fact that Ref. [1] is based on a NLO calculation in the Coulomb gauge. In this gauge the collinear and collinear-soft singularities are entirely contained in the cut self-energy graphs. Thus we simply eliminate the small-virtuality part of cut self-energy subgraphs in \mathcal{B}_s^{B+1} graphs and instead incorporate these contributions into the primary parton splittings from the corresponding \mathcal{B}_s^B graph. One could subtract a different quantity from the \mathcal{B}_s^{B+1} graphs as long as it has the same collinear and collinear-soft singularities,⁵ as in the work of Refs. [3, 4].

The next step, and the main subject of this paper, is to treat the soft, wide angle singularities of the theory. Again, we subtract terms with these singularities from the \mathcal{B}_s^{B+1} graphs and then incorporate them as radiation from the \mathcal{B}_s^B graphs. Here, the hard partons emerging from an \mathcal{B}_s^B scattering form an antenna that radiates the soft gluon. The gluon is radiated coherently from the antenna and is not part of any jet.

This gives an algorithm that can be viewed as a simulation of the production of three hard partons (for the three jet process considered in this paper) and one soft gluon, with each of the three hard partons splitting into two daughter partons. The six daughter partons and one soft gluon then serve as the progenitors of parton showers according to the simple algorithm used in Ref. [1] or any standard algorithm. There remains the remnants of the order \mathcal{B}_s^{B+1} graphs, with three and four parton final states. Each of these final state partons serves as the progenitor of whatever sort of parton shower is desired.

The results of this paper suggest a strategy for building future NLO calculations matched to parton showers. The matching concerns the primary parton splittings, that is the first splittings of the partons emerging from a Born graph. The matching also needs the radiation

⁵ This might, however, require adjustment of the treatment of the soft gluon singularities presented in this paper.

of a soft gluon from the antenna formed by partons emerging from the Born graph. This suggests that the author of an NLO calculation might build in the primary parton splittings and the soft gluon radiation. There are also secondary splittings. These are the splittings from the soft gluon produced from a Born graph, the splittings of the daughters produced by the primary splittings, the splittings of the partons from an order $\frac{B+1}{s}$ graph, and, finally, the further splittings of all of these partons as a complete parton shower is formed. The secondary splittings do not need to be matched to the NLO calculation. That is, the soft gluon and the partons after the primary splittings and the partons produced by the $\frac{B+1}{s}$ graphs can be fed to any shower and hadronization algorithm as long as it is infrared safe. The result is that for a given process such as $e^+ + e^- \rightarrow 3$ jets we can have N_{NLO} next-to-leading order calculations and N_{MC} shower and hadronization calculations and we do not need $N_{\text{NLO}} - N_{\text{MC}}$ matching schemes as long as each NLO calculation includes its primary parton splittings and treatment of soft gluon radiation.

This does not preclude debate over how best to do the primary parton splitting and soft gluon radiation. This paper and Ref. [1] have, of necessity, chosen one scheme, but that scheme may well be less than optimal.

The code described in this paper is available at [14].

Acknowledgments

The author is pleased to thank his collaborator on Ref. [1], Michael Kramer, for his advice. In addition, Steve Mrenna, John Collins, Torbjorn Sjstrand, George Sterman, and Michael Seymour provided helpful advice and criticisms.

APPENDIX : THE INTEGRATION FOR VIRTUAL SOFT GLUONS

We have seen that in order to calculate the contribution to I from an order $\frac{2}{s}$ graph with a virtual loop, we should calculate a difference integral of the form

$$\int_{\mathcal{Q}_1}^Z \int_{\mathcal{Q}_2}^Z \int_{\mathcal{Q}_3}^Z \int_{\mathcal{Q}_k}^X \int_{\mathcal{Q}_B}^Z d^3\Gamma f(\Gamma; \mathcal{Q}_1; \mathcal{Q}_2; \mathcal{Q}_3) \\ \times \int_{fi;jg}^Z \frac{d^3\Gamma^0}{2\mathcal{J}^0} \left(\frac{p^2}{M_{\text{soft}}^2} \right) \frac{s}{2} F_{ij}^J(\Gamma^0; \mathcal{Q}_1; \mathcal{Q}_2; \mathcal{Q}_3) R_0(\mathcal{Q}_1; \mathcal{Q}_2; \mathcal{Q}_3) ; \quad (\text{A } 1)$$

where J is L or R and F_{ij}^L and F_{ij}^R are given in Eqs. (45) and (46). In this Appendix, we consider $J = L$, that is a virtual loop to the left of the final state cut. The integrand for the original graph is represented here by the function f . The momenta \mathcal{Q}_i are the momenta of the final state partons, while Γ is the momentum in the virtual loop. There are either one or two terms in the sum over the indices $fi;jg$, depending on the graph. The term $fi;jg$ is included if there is a potentially soft virtual gluon connecting final state lines i and j in f . Let \mathcal{I}_{ij} be that combination of Γ and the \mathcal{Q}_k that is carried by this potentially soft virtual line in f . For example if the final state propagators 1 and 2 are connected by a gluon line that carries momentum l in the virtual loop and propagators 2 and 3 are also connected by a virtual gluon line that carries momentum $l - \mathcal{Q}_2$, then $\mathcal{I}_{12} = \Gamma$ and $\mathcal{I}_{23} = \Gamma - \mathcal{Q}_2$. In the virtual subtraction term, we call the integration variable Γ^0 . If we identify Γ^0 with \mathcal{I}_{ij} , the F_{ij} subtraction term matches f when $\mathcal{I}_{ij} \rightarrow 0$, so that the leading singularity is cancelled.

The method used in this paper is to perform the virtual loop integrations numerically, as in [2, 10, 12] and [1]. Thus we must make sure that this cancellation works numerically. First, we define the dependence of f and R on $\epsilon_1; \epsilon_2; \epsilon_3$ to be the dependence computed from the relevant Feynman graphs with the final state momenta $q_1; q_2; q_3$ on-shell: $q_k^2 = 0$. Of course, in our present discussion, the q_k are the momenta of on-shell massless partons, so evidently $q_k^2 = 0$. However, at a later stage in the calculation each of these partons will generate a parton shower with the same ϵ . Even with a shower, we take the functions f and R to remain unchanged. This is in contrast to our treatment of showering from the Born graphs and is required for the NLO graphs in order to preserve the soft gluon cancellations.

Next, in the integral of the full graph f , the integration is deformed⁶ into complex loop-momentum space,

$$\int_Z d^3 \mathbb{L} J(\mathbb{L}) f(\mathbb{L} + i\epsilon; \epsilon_1; \epsilon_2; \epsilon_3) : \quad (\text{A } 2)$$

The imaginary part of the deformed loop momentum is a definite function $\sim(\mathbb{L})$ of the real part. The jacobian J is the determinant of the matrix $(\partial_{\mathbb{L}^j} + i\partial_{\mathbb{L}^j} \sim)$. By deforming the contour, we avoid the singularity of the form

$$\frac{1}{\mathbb{P}_{ij} + \mathbb{P}_{ij} \sim \mathbb{P}_{ij} + \mathbb{L}_{ij} + i\epsilon_j \sim \mathbb{P}_{ij} \mathbb{L}_{ij} \sim i\epsilon_j + i} \quad (\text{A } 3)$$

in f , the $fi; jg$ scattering singularity. It is, however, not allowed to deform the contour away from the soft singularity at $\mathbb{L}_{ij} = 0$. For that reason $\sim(\mathbb{L})$ is proportional to \mathbb{L}_{ij}^2 as $\mathbb{L}_{ij} \rightarrow 0$. Hence we come very near to the scattering singularity when \mathbb{L}_{ij} is small.

What about the subtraction term? Here there is a singularity of the form

$$\frac{1}{\mathbb{T}^0 (\epsilon_1 \epsilon_2) + i} : \quad (\text{A } 4)$$

We may call this the approximate scattering singularity. We note that

$$\mathbb{P}_{ij} + \mathbb{P}_{ij} \sim \mathbb{P}_{ij} + \mathbb{L}_{ij} \sim \mathbb{P}_{ij} \mathbb{L}_{ij} \sim \mathbb{L}_{ij} (\epsilon_1 \epsilon_2) \quad (\text{A } 5)$$

for $\mathbb{L}_{ij} \rightarrow 0$, so the singularity (A.4) is indeed an approximation to (A.3) if we identify \mathbb{T}^0 with \mathbb{L}_{ij} . As in the f integral, we need to deform the contour to avoid the singularity (A.4). As in the f integral, the deformation will have to vanish as we approach the soft singularity at $\mathbb{T}^0 = 0$. In order for the cancellation between the full graph and the soft gluon subtraction to work, we need to be careful about the matching of the singularities in the two integrands.

We are now in a position to state the matching problem more precisely. We define complex vectors s_{ij} , one for each potentially soft gluon line $fi; jg$ in Eq. (A.1). Each s_{ij} is a function of the corresponding \mathbb{L}_{ij} that is asymptotically equal to \mathbb{L}_{ij} when \mathbb{L}_{ij} is small. Then we write the integral in Eq. (A.1) in the form

$$\int_Z d\epsilon_1 \int_Z d\epsilon_2 \int_Z d\epsilon_3 \int_X \epsilon_1 \int_Z d^3 \mathbb{L} J(\mathbb{L}) f(\mathbb{L} + i\epsilon; \epsilon_1; \epsilon_2; \epsilon_3) \\ \int_{ij}^X \frac{J_s(\mathbb{L}_{ij})}{2 \mathbb{P}_{ij}^3} (\mathbb{L}_{ij}^2 < M_{\text{soft}}^2) \frac{s}{2} F_{ij}^J(s_{ij}; \epsilon_1; \epsilon_2; \epsilon_3) R_0(\epsilon_1; \epsilon_2; \epsilon_3) : \quad (\text{A } 6)$$

⁶ Some relevant theorems concerning contour deformations in more than one dimension are given in [11]

The jacobian J_s is the determinant of the matrix $\partial s_{ij}^I = \partial \mathbb{I}_{ij}^J$. Our goal will be to specify the functions s_{ij} so that we avoid the approximate scattering singularity in the second term of Eq. (A.6) and so that the $\mathbb{I}_{ij} \neq 0$ singularities in the sum of the two terms cancel sufficiently well that the integral is convergent.

We will approach this problem in stages. First, we concentrate on the $\mathbb{I}_{ij} \neq 0$ region.

We immediately recognize a small problem. The soft singularity (with $\sim = 0$) lies on an ellipse, while the approximate soft singularity lies on a plane. To make them match at the required accuracy, we define

$$s_{ij} = \mathbb{I}_{ij} + (1 - \frac{\mathbb{I}_{ij}^2}{M_{\text{soft}}^2})^n \tilde{\mathbb{I}}_{ij} + i\tilde{\mathbb{I}}_{ij} \quad (\text{to be improved}); \quad (\text{A.7})$$

where $\tilde{\mathbb{I}}$ and $\tilde{\mathbb{I}}$ are certain functions of \mathbb{I}_{ij} to be defined below and M_{soft}^2 is the maximum value of \mathbb{I}^2 in the soft gluon subtraction, Eq. (14).

The idea is to have the soft subtraction cancel the leading singular behavior of f point by point in \mathbb{L} . To do this, we need to match the singularity

$$\frac{1}{D_0(\mathbb{I}_{ij} + i\tilde{\mathbb{I}})} = \frac{1}{\mathfrak{F}_{ij} + \mathfrak{F}_{ij} \mathfrak{F}_{ij} + \mathfrak{F}_{ij} + \mathbb{I}_{ij} + i\tilde{\mathbb{I}} \mathfrak{F}_{ij} \mathfrak{F}_{ij} \mathbb{I}_{ij} + i\tilde{\mathbb{I}} \mathfrak{F}_{ij}} \quad (\text{A.8})$$

in f with the singularity

$$\frac{1}{D_s(s_{ij})} = \frac{1}{s_{ij} (\hat{\mathcal{Q}}_i \hat{\mathcal{Q}}_i)} \quad (\text{A.9})$$

in F_{ij} .

There are three parts in the relation (A.7) between s_{ij} and \mathbb{I}_{ij} . There is a real displacement $\tilde{\mathbb{I}}$, a contour deformation $\tilde{\mathbb{I}}$ in the imaginary direction, and a factor $(1 - \frac{\mathbb{I}_{ij}^2}{M_{\text{soft}}^2})^n$. The factor $(1 - \frac{\mathbb{I}_{ij}^2}{M_{\text{soft}}^2})^n$ serves to set the deformation to zero at the edge of the integration region and needs no further discussion. We choose the real displacement to be

$$\tilde{\mathbb{I}}_{ij} = \frac{\mathbb{I}_{ij}^2}{2\mathfrak{F}_{ij}\mathfrak{F}_{ij} + \mathfrak{F}_{ij} + \mathfrak{F}_{ij}} \frac{1}{\hat{\mathcal{Q}}_i \hat{\mathcal{Q}}_i} \frac{1}{\hat{\mathcal{Q}}_j \hat{\mathcal{Q}}_j} : \quad (\text{A.10})$$

This choice is motivated by carrying out the expansion (A.4) to one more order. Then one finds that

$$(\mathbb{I}_{ij} + \tilde{\mathbb{I}}_{ij}) (\hat{\mathcal{Q}}_i \hat{\mathcal{Q}}_i) \mathfrak{F}_{ij} + \mathfrak{F}_{ij} \mathfrak{F}_{ij} \mathfrak{F}_{ij} + \mathbb{I}_{ij} \mathfrak{F}_{ij} \mathfrak{F}_{ij} \mathbb{I}_{ij} + O(\mathbb{I}_{ij}^3) : \quad (\text{A.11})$$

The imaginary displacement is

$$\tilde{\mathbb{I}}(\mathbb{I}) = C \mathbb{I}^2 \ln(1 + \hat{\mathcal{Q}}_i; 1 + \hat{\mathcal{Q}}_j (\hat{\mathcal{Q}}_j \hat{\mathcal{Q}}_j)) : \quad (\text{A.12})$$

Here C is a parameter with dimensions of inverse momentum. This function matches the function $\tilde{\mathbb{I}}(\mathbb{I})$ in the limit of small \mathbb{I} as long as one chooses C to be the same parameter as is used in $\tilde{\mathbb{I}}(\mathbb{I})$.⁷ Thus

$$D_s(s_{ij}) = D_0(\mathbb{I}_{ij} + i\tilde{\mathbb{I}}) + O(\mathbb{I}_{ij}^3) : \quad (\text{A.13})$$

⁷ Specifically, $C = 2 \ln(1 + \mathfrak{F}_{ij} + \mathfrak{F}_{ij} \mathfrak{F}_{ij} + \mathfrak{F}_{ij} + \mathfrak{F}_{ij})$, where \mathfrak{F}_{ij} and \mathfrak{F}_{ij} are the parameters used to define the deformation in [11].

Now we have two methods for moving the integration contour, each of which works in its region and turns on in the region of the other method. All that we have to do is to add the two deformations,

$$s_{ij} = \mathcal{I}_{ij} + (1 - \mathcal{I}_{ij}^2 M_{\text{soft}}^2)^n \tilde{\mathcal{I}}_{ij} + i \tilde{\mathcal{I}}_{ij}^o + \tilde{\mathcal{I}}_{ij} \quad (\text{A } 21)$$

This is the nal prescription, with $\tilde{\mathcal{I}}_{ij}$ given in Eq. (A 10), $\tilde{\mathcal{I}}_{ij}^o$ given in Eq. (A 12), and $\tilde{\mathcal{I}}_{ij}$ given in Eq. (A 20).

- [1] M. Kramer and D.E. Soper, [arXiv:hep-ph/0306222].
- [2] M. Kramer and D.E. Soper, Phys. Rev. D 66, 054017 (2002) [arXiv:hep-ph/0204113].
- [3] S. Frixione and B.R. Webber, JHEP 2606, 029 (2002) [arXiv:hep-ph/0204244].
- [4] S. Frixione, P. Nason and B.R. Webber, JHEP 0308, 007 (2003) [arXiv:hep-ph/0305252].
- [5] T. Sjstrand, Comput. Phys. Commun. 39 (1986) 347; T. Sjstrand, P. Eden, C. Friberg, L. Lonnblad, G. Miu, S. Mrenna and E. Norrbin, Comput. Phys. Commun. 135, 238 (2001) [arXiv:hep-ph/0010017].
- [6] G. Marchesini, B.R. Webber, G. Abbiendi, I.G. Knowles, M.H. Seymour and L. Stanco, Comput. Phys. Commun. 67, 465 (1992); G. Corcella et al., JHEP 0101 010 (2001) [arXiv:hep-ph/0011363].
- [7] L. Lonnblad, Comput. Phys. Commun. 71, 15 (1992).
- [8] H. Baer and M.H. Reno, Phys. Rev. D 45, 1503 (1992); S. Mrenna, [arXiv:hep-ph/9902471]; B. Potter, Phys. Rev. D 63, 114017 (2001) [arXiv:hep-ph/0007172]; M. Dobbbs, Phys. Rev. D 64, 034016 (2001) [arXiv:hep-ph/0103174]; B. Potter and T. Schomer, Phys. Lett. B 517, 86 (2001) [arXiv:hep-ph/0104261]; M. Dobbbs, Phys. Rev. D 65, 094011 (2002) [arXiv:hep-ph/0111234]; Y. Kurihara, J. Fujimoto, T. Ishikawa, K. Kato, S. Kawabata, T. Munehisa and H. Tanaka, Nucl. Phys. B 654 (2003) 301 [arXiv:hep-ph/0212216].
- [9] J.C. Collins, JHEP 0005, 004 (2000) [arXiv:hep-ph/0001040]; J.C. Collins and F. Hautmann, JHEP 0103, 016 (2001) [arXiv:hep-ph/0009286]; Y. Chen, J.C. Collins and N. Tkachuk, JHEP 0106, 015 (2001) [arXiv:hep-ph/0105291]; J.C. Collins and X. Zu, JHEP 0206, 018 (2002) [arXiv:hep-ph/0204127].
- [10] D.E. Soper, Phys. Rev. Lett. 81, 2638 (1998) [arXiv:hep-ph/9804454].
- [11] D.E. Soper, Phys. Rev. D 62, 014009 (2000) [arXiv:hep-ph/9910292].
- [12] D.E. Soper, Phys. Rev. D 64, 034018 (2001) [arXiv:hep-ph/0103262].
- [13] G. Grammer and D.R. Yennie, Phys. Rev. D 8, 4332 (1973). See also J.C. Collins and D.E. Soper, Nucl. Phys. B 193, 381 (1981).
- [14] D.E. Soper, beowulf Version 3.0, <http://zebu.uoregon.edu/~soper/beowulf/>.